A method for ab initio nonlinear electron-density evolution

Roi Baer, and Recca Gould

Citation: The Journal of Chemical Physics **114**, 3385 (2001);
View online: https://doi.org/10.1063/1.1342761
View Table of Contents: http://aip.scitation.org/toc/jcp/114/8
Published by the American Institute of Physics

A method for *ab initio* nonlinear electron-density evolution

Roi Baer[a] and Recca Gould
Department of Physical Chemistry and The Lise Meitner Minerva-Center for Quantum Chemistry, The Hebrew University of Jerusalem, Jerusalem 91904, Israel

(Received 15 August 2000; accepted 1 December 2000)

A numerical method is given for effecting nonlinear local density functional evolution. Within a given time interval, Chebyshev quadrature points are used to sample the evolving orbitals. An implicit equation coupling wave functions at the different time points is then set up. The equation is solved iteratively using the ''direct inversion in iterative space'' acceleration technique. Spatially, the orbitals are represented on a Fourier grid combined with soft pseudopotentials. The method is first applied to the computation of the $^3\Pi_g$ adiabatic potential energy curves of Al_2. Next, the electronic dynamics of a toy molecular wire is studied. The wire consists of a C_2H_4 molecule connected via sulfur atoms to two gold atoms, the ''electrodes.'' The molecule is placed in a homogeneous electric field and a dynamical process of charge transfer is observed. By comparing the transient with that of a resistance-capacitance circuit, an effective Ohmic resistance and capacitance is estimated for the system. © *2001 American Institute of Physics.*
[DOI: 10.1063/1.1342761]

I. INTRODUCTION

A fundamental problem of theoretical chemistry is to accurately account for the dynamics of electrons and nuclei in molecules. This challenge is beyond the reach of present computational capabilities, so simplifying approximations must be made. The fact that nuclei are thousands of times heavier than electrons is exploited and the dynamics of the two entities are thus treated separately. We focus in this article on the fast electron dynamics.

Even with fixed nuclei, exerting a stationary potential V_N on the electrons, it is impractical to demand a detailed description of the electronic motion. Instead, a reduced account is adopted, limited to the study of the evolution of the one-electron density. The time-dependent density functional theory (TDDFT), developed by Runge and Gross,[1] is a general framework with which this is achieved. In TDDFT, within a Kohn–Sham[2] approach, the time-dependent electron density is written as

$$\rho(\mathbf{r},t)=\sum_{n=1}^{N_e}|\psi_n(\mathbf{r},t)|^2, \tag{1}$$

where N_e is the number of electrons. The evolution of the N_e single electron Kohn–Sham (KS) orbitals $\psi_n(\mathbf{r},t)$ is determined by a time-dependent variational principle applied to the KS energy

$$E\{\psi_n\}=\sum_{n=1}^{N_e}\langle\psi_n|K|\psi_n\rangle+\sum_{n=1}^{N_e}\langle\psi_n|V_N|\psi_n\rangle + \frac{e^2}{2}\int\int\frac{\rho(\mathbf{r}',t)\rho(\mathbf{r},t)}{|\mathbf{r}-\mathbf{r}'|}d^3r'\,d^3r+E_{xc}\{\rho\}. \tag{2}$$

Here, the first term is the kinetic energy of noninteracting electrons in the KS orbitals; the second is the corresponding energy of electron–nuclei interaction. The third term is the direct Coulomb repulsion energy of the density $\rho(\mathbf{r},t)$. Finally, the last term, also a functional of $\rho(\mathbf{r},t)$, accounts for all the residual many-body energetics, such as exchange and correlation. This leads to the following set of N_e equations of motion for the Kohn–Sham orbitals:

$$i\hbar\frac{\partial\psi_n(\mathbf{r},t)}{\partial t}=H(\psi(\mathbf{r},t))\psi_n(\mathbf{r},t),\ n=1,\ldots,N_e, \tag{3}$$

where the Hamiltonian operator is dependent on the KS orbitals. Within the local density approximation,[2] the exchange correlation takes a simple form, $E=\int\rho\varepsilon(\rho)d^3r$ and one can write the Hamiltonian of the electronic system as

$$H=-\frac{\hbar^2}{2\mu_e}\nabla^2+V_N(\mathbf{r})+e^2\int\frac{\rho(\mathbf{r}')}{|\mathbf{r}-\mathbf{r}'|}d^3\mathbf{r}'+V_{xc}(\rho(\mathbf{r})), \tag{4}$$

where $V_{xc}(\rho)=\varepsilon(\rho)+\rho\varepsilon'(\rho)$. Equations (3) and (4) constitute a set of nonlinearly coupled Schrödinger-type equations.

This paper develops a method for computing the nonlinear evolution of an initial KS orbital configuration in time. The nonlinearity of the equations makes a solution considerably more difficult than the case of linear evolution.

A numerical scheme for solving the nonlinear Schrödinger equation must simultaneously address time evolution and spatial representation of the wave functions and operators. These two topics are interrelated and should be applied in a balanced way. When global methods such as Fourier-grid or plane waves[3] are applied for the spatial representation, a matching high-precision time evolution method must follow. The usual differential equation methods, such as adaptive Runge–Kutta, and Adams–Bashforth–Moulton predictor–corrector schemes (see Ref. 4 for discussion), as

[a]Electronic mail: roib@fh.huji.ac.il

well as more recent and specialized techniques[4–6] are low order in time step. Using these methods within a high-quality spatial representation leads to an unbalanced overall treatment. This problem was recognized by Miyamoto *et al.*, who recently developed a high-order split operator method for treating this problem.[7]

An example of a global evolution method, a perfect match for the high-quality spatial representation of the Fourier grid,[8] is the method of Kosloff.[9] However, this approach is limited to the *linear* Schrödinger equation because it exploits the closed form of the evolution operator, $\psi(t)=e^{-iHt/\hbar}\phi$, which is expanded by a series of Chebyshev polynomials. Via the $t-t'$ formalism[10–12] or a Lanczos subspace propagation,[13,14] the Kosloff method was extended to time-dependent Hamiltonians. However, these extensions still rely on the linearity of the basic equations.

The evolution method we present below also exploits the power of Chebyshev polynomials. However, here it is done in such a way that a closed form for the evolution operator is not needed so that nonlinear and explicitly time-dependent Hamiltonians can be treated. We achieve this by performing the Chebyshev interpolation *in the time domain* instead of the energy domain, as effectively done in the Kosloff method.[3] This alternative treatment is flexible enough to treat both time dependent and nonlinear Hamiltonians.

The approach is based on a recently published nonlinear solver for the Gross–Pitaevskii equations describing the mean-field dynamics of Bose Einstein condensates.[15] It is in some ways similar to the well-known Adams–Moulton (AM) method,[16] but is critically different in two aspects. The AM method relies on *extrapolation* and uses equally spaced points in the time domain. Contrariwise, the method presented here relies on *interpolation* and uses Chebyshev sampling points in the time domain. These differences allow the achievement of highly accurate results.

The fundamentals of the method are explained in Sec. II. In Secs. III and IV, its capabilities are demonstrated by computing the excitation energies of triplet Al_2 followed by an application to a molecular wire model.

II. METHOD

The following integral equation is equivalent to the time-dependent Schrödinger equation [Eq. (3)]:

$$\psi_n(t)=\phi_n-i\hbar^{-1}\int_0^t \hat{H}(\{\psi(\tau)\},\tau)\psi_n(\tau)d\tau. \tag{5}$$

A global representation for time dependence within a given interval $[0,T]$ is now constructed

$$\psi_n(t)=\sum_{k=0}^{N-1}\psi_n(t_k)Q_k(t), \tag{6}$$

where the N sampling points t_k and interpolation functions $Q_k(t)$ are independent of $\psi_n(t)$. Plugging this into Eq. (5), one can write

$$\psi_n(t_m)=\phi-i\frac{T}{\hbar}\sum_{l=0}^{N-1}\hat{H}(\psi(t_l),t_l)\psi_n(t_l)I_{lm}, \tag{7}$$

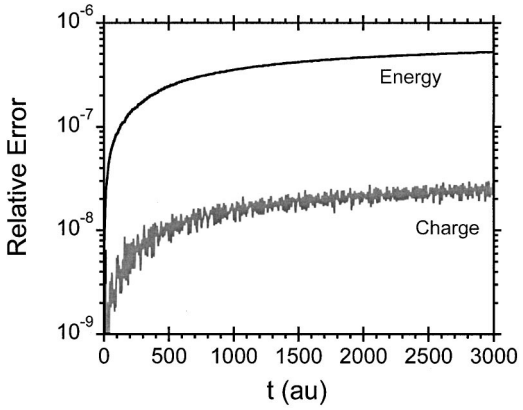

FIG. 1. Numerical error vs propagation time for the Al_2 computation. The error is estimated from the relative deviance from energy and charge conservation.

where

$$I_{lm}=\frac{1}{T}\int_0^{t_l}Q_m(\tau)d\tau. \tag{8}$$

Equation (7) is an implicit equation on the values of the wave function at the set of discrete points. Once this equation is solved, the values at the sampling points are used to represent the entire time dependence via Eq. (6).

The N sampling points t_n are chosen as Chebyshev quadrature points. Thus, the interval $[0,T]$ is mapped to the interval $[-1,1]$ by $x=(2t/T)-1$ and the sampling points are the roots of the Chebyshev polynomial of order N

$$t_n=T(1+x_n)/2,\ n=0,1,\ldots,N-1, \tag{9}$$

where x_n are defined in the Appendix [Eq. (A8)], where a more complete account of the details of the theory, including an explicit form for the functions $Q_n(t)$, is given.

The implicit Eq. (7) is solved by setting $\psi_n^0(t_l)=e^{-iHt_l/\hbar}\phi_n$ effected using Kosloff evolution,[9] and then performing the following iterations to convergence:

$$\psi^{L+1}(t_m)=\phi-i\frac{T}{\hbar}\sum_{n=0}^{N-1}\hat{H}(\psi^L(t_n),t_n)\psi^L(t_n)I_{nm}. \tag{10}$$

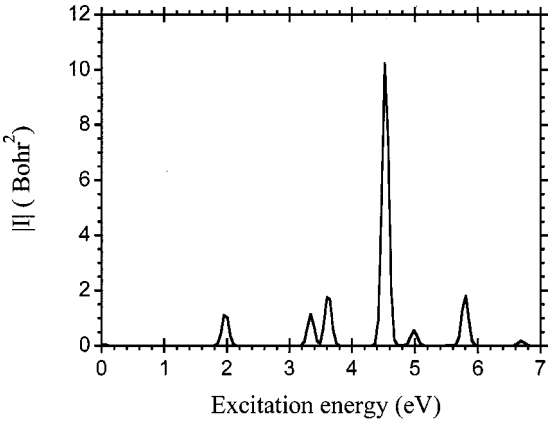

FIG. 2. The dipole excitation spectrum of triplet Al_2 by the time-dependent LDA method. The transform parameters are: $T=3300$ a.u.; $\sigma=525$ a.u.; $t_o=1650$ a.u.

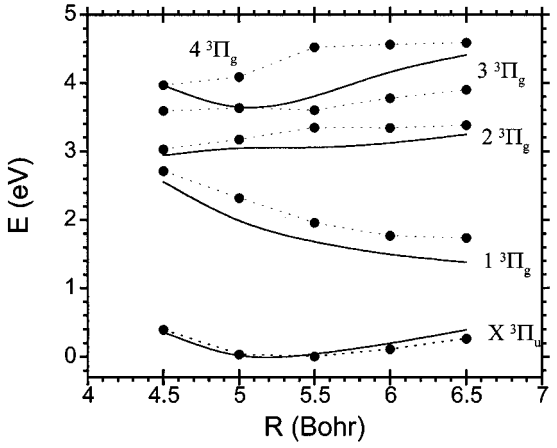

FIG. 3. Adiabatic potential energy curves for Al_2, computed by TDLDA. The solid lines are the results of Ref. 30. The filled circles are the results of the present computation (connected by dotted lines as guides to the eye).

Convergence is accelerated by using the technique of direct inversion in iterative space (DIIS).[17] An important issue is the number of sampling points N. It can be shown that this is determined by[15]

$$N=\frac{e}{4}\Omega T+N_r, \tag{11}$$

where Ω is the largest temporal frequency in the electronic density, estimated as the largest eigenvalue of the Hamiltonian. The integer N_r lies between 3 to 10, depending on the required accuracy.[15]

III. ELECTRONIC EXCITATIONS

As a demonstration of the method, we apply it to the computation of electronic excitation energies of the aluminum dimer. Recently, several authors have published successful applications of linear response versions of TDLDA to compute excitation energies,[18,19] yielding excitation energies usually within a few electron volts of the experimental results. The idea of using TDLDA in real time for computing the excitation energies, without invoking linear response theory, was first put forward by Yabana and Bertsch.[20] This approach has been used in several studies.[21–24] A slightly different way of extracting the excitation energies from the time-dependent signal is taken here.

TABLE I. Low-lying vertical-parallel excitation energies (eV) of Al_2 (at 5.3 bohr). The results are compared with experimental and other theoretical estimates.

	Matrix (Ref. 26)	Absorption (Ref. 25)	Emission (Ref. 27)	Ref. 29	Ref. 30	TDLDA
$1\,^3\Pi_g$		1.86	repuls.	1.85	1.88	2.1
$2\,^3\Pi_g$	3.03			3.03	3.06	3.2
$E'\,3^3\Pi_g$		3.48		3.49	3.57	3.6
$G\,^3\Pi_g$		4.28	4.28			4.3

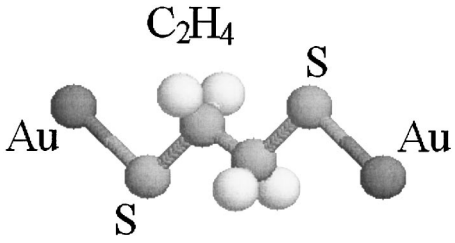

FIG. 4. A model molecular wire where the ethylene molecule is connected via sulfur atoms to the leads, modeled as gold atoms.

A. Computing excitation energies

The ground-state density is perturbed by issuing a momentum kick to all orbitals[20]

$$\psi_n(\mathbf{r})=e^{i\mathbf{k}\cdot\mathbf{r}}\psi_n^{\mathrm{GS}}(\mathbf{r})\approx(1+i\mathbf{k}\cdot\mathbf{r})\psi_n^{\mathrm{GS}}(\mathbf{r}), \tag{12}$$

where $k=|\mathbf{k}|$ is small. This excites only dipole-coupled modes. Other modes can be excited by designing additional types of perturbations, and analyzing the dynamics in a similar way shown below. The response to this perturbation is determined by accurately following the time evolution of the electronic density, recording the dipole moment signal

$$\mathbf{D}(t)=e\int \mathbf{r}\rho(\mathbf{r},t)d^3r. \tag{13}$$

For simplicity, let us examine the signal in the direction of the kick x (so-called parallel excitations). The accurate dipole signal in the x direction is composed of frequencies corresponding to the excitation energies $\hbar\omega_{n0}=E_n-E_{\mathrm{GS}}$, given by

$$\begin{aligned} d(t)&=e\langle\Psi_{\mathrm{GS}}|e^{-ik\hat{x}}e^{i\hat{H}t}\hat{x}e^{-i\hat{H}t}e^{ik\hat{x}}|\Psi_{\mathrm{GS}}\rangle \\ &=e\left[x_{00}+2k\sum_n |x_{0n}|^2\sin(\omega_{n0}t)\right]+O(k^2), \end{aligned} \tag{14}$$

where $e\hat{x}=e\Sigma_{m=1}^{N_e}\hat{x}_m$ is the electron dipole operator in the x direction, and $x_{n0}=\langle\Psi_n|\hat{x}|\Psi_{\mathrm{GS}}\rangle$ is the transition dipole element. Here, we designate by Ψ the exact electronic eigenstates. The LDA-based evolution yields an approximate dipole signal, and the ground-state excitations ω_{n0} and transition dipole magnitudes can thus be determined by Fourier analyzing the signal. For a component of the signal $d(t)$ of length $0<t<T_f$, define the following transform:

TABLE II. Cartesian coordinates (a.u.) of the atoms in the model molecular wire. The number of valence electrons explicitly treated is also shown.

Atom	X	Y	Z	Electrons
Au1	0.00	0.15	−7.46	11
S1	0.00	−2.10	−3.53	6
C1	0.00	0.51	−1.34	4
H1	1.68	1.66	−1.64	1
H2	−1.68	1.66	−1.64	1
C2	0.00	−0.49	1.36	4
H3	1.68	−1.64	1.66	1
H4	−1.66	−1.64	1.66	1
S2	0.00	2.12	3.55	6
Au2	0.00	−0.13	7.48	11

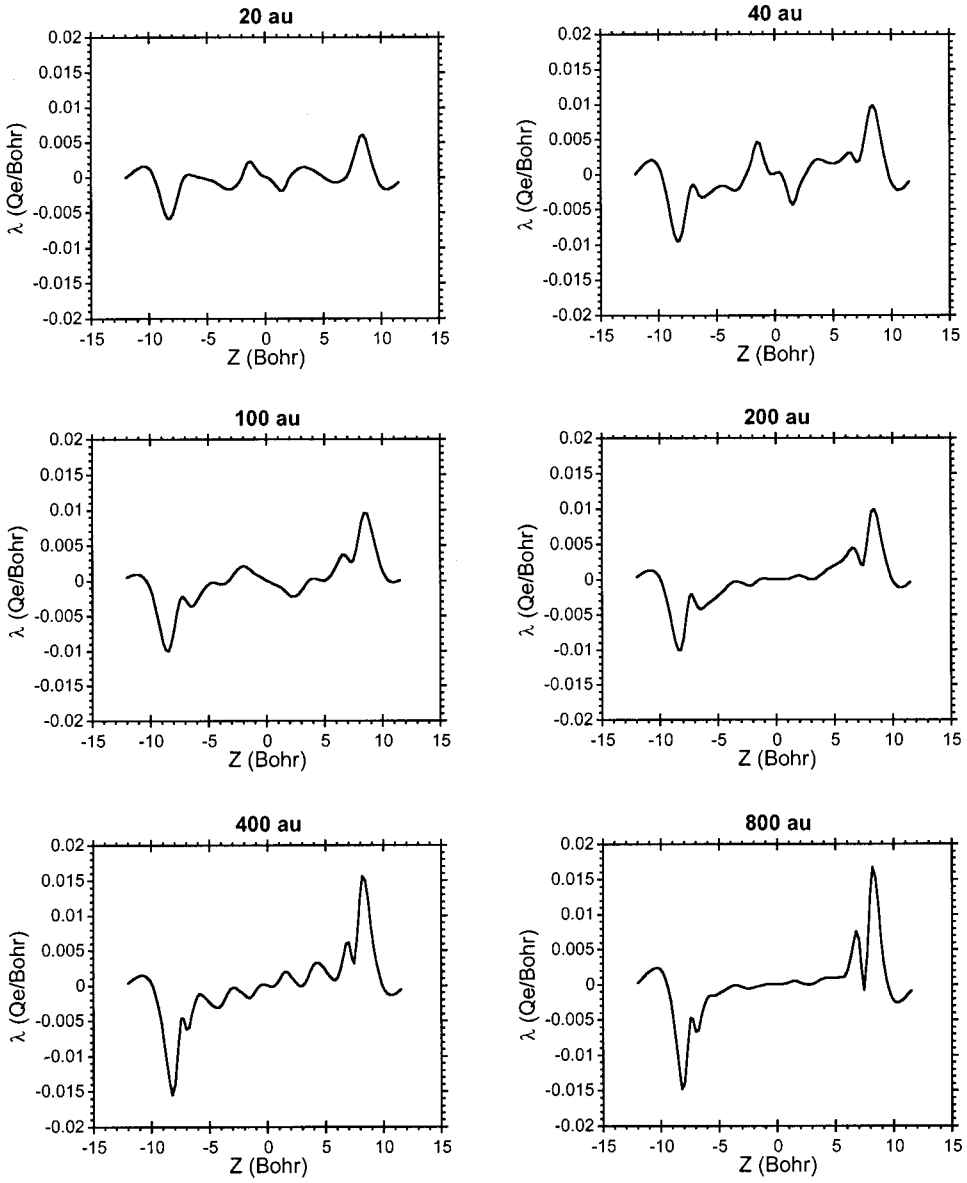

FIG. 5. Temporal snapshots of the linear charge density $\lambda(z,t)=\int\int \delta\rho(\mathbf{r},t)dx\,dy$, where $\delta\rho(t)=\rho(t)-\rho(0)$.

$$I(\omega)=\frac{1}{\sqrt{2\pi}\sigma e k_x}\int_{-\infty}^{\infty} e^{-[(t-t_o)^2/2\sigma^2]}e^{-i\omega t}[d(t)-\bar{d}]dt, \tag{15}$$

with $t_o=T_f/2$ and $\sigma \ll T_f$ (thus, the integral limits can be extended to infinity). When σ and T_f are large, the components of the spectrum are well resolved and nonoverlapping, and the function $|I(\omega)|$ becomes

$$|I(\omega)| \overset{\text{large } \sigma \ll T_f}{\longrightarrow} \sum_n |x_{n0}|^2 e^{-(1/2)\sigma^2(\omega-\omega_{n0})^2} \tag{16}$$

The interpretation of the spectrum $|I(\omega)|$ is that each resolved peak corresponds to an excitation frequency and the peak height is related to the transition dipole moment, given by

$$|d_{n0}|^2=e^2|I(\hbar\omega_{\text{peak}}=E_{n0})|. \tag{17}$$

B. Vertical-parallel excitations of Al_2

We now apply this method and compute the Al_2 excitation spectrum. This system is a nontrivial test case because long propagation times are needed for resolving the small energy differences. For comparison with experiment and other theoretical treatments, there are several sources, experimental[25–27] and theoretical.[28–30]

The computation treats explicitly the 6 valence electrons, where the wave functions are represented on a three-dimensional grid spanning a cubic $20\times20\times20$ bohr^3 box. Core electrons are eliminated using a norm conserving Troulier–Martins[31] LDA-based pseudopotential, generated by the FHI98PP[32] package.

A spin-polarized time-independent LDA computation was first performed, for determining the ground-state density and properties. The common experimental and theoretical wisdom, that the Al_2 ground state is a $^3\Pi_u$ state, was ascertained. We then computed the ground-state energy curve of Al_2 and performed a nuclear wave-packet computation, for

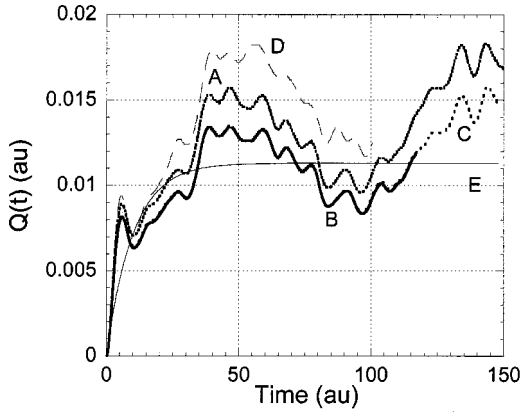

FIG. 6. The charge transferred from the right part to the left part of the molecule as a function of time. Shown, the calculated transients (A–D) and the *RC*-circuit transient (E) discussed in the text. The latter is fitted to the data of curves C and D. The grid parameters for the A–D transients are given in Table III.

TABLE III. The resistance and capacitance of the MW as determined by the *RC* model from the *ab initio* data for various grid spacings (δx) and box dimensions ($12\times12\times$Lz bohr^3).

	Lz (bohr)	δx (bohr)	$R\cdot C$ (a.u.)	R (kΩ)	C (10^{-20} F)
A	28	0.50	10.1	50.0	0.5
B	28	0.40	10.0	55.0	0.5
C	28	0.33	10.0	55.0	0.5
D	32	0.40	12.6	51.0	0.6

determining the vibrational spectroscopic properties. We find that in the $v=0$ vibrational state, the Al_2 bond length is $R=2.81$ Å and the $0\rightarrow1$ vibrational transition energy is 238 cm^{-1}. As is common with LDA, when compared to experiment[25] and recent *ab initio* computations,[30] the bond length is overestimated, with a discrepancy of 0.07 Å. The LDA vibrational frequency is underestimated (by 40 cm^{-1}).

With the ground-state density at hand, the TDDFT computation is carried out. The time step was $T=0.1$ a.u., sampled with $N=6$ Chebyshev points. The high accuracy and stability of the numerical evolution method is evident from an inspection of Fig. 1, where it is seen that the relative numerical error (as estimated from violation of energy and charge conservation) is small and its accumulation rate is sublinear in time.

The dipole signal yields an excitation spectrum as shown in Fig. 2, for a dimer separation of $R=5.5$ bohr. The resolved lines are Gaussian in shape with height indicative of the transition dipole moment [see Eq. (17)]. Repeating the computation for several bond lengths, it is possible to obtain adiabatic potential curves as shown in Fig. 3 and compared to the corresponding computations of Ref. 30. In Table I, a comparison of the vertical excitation energies with theoretical and experimental data is made. It is seen that for the lower transitions, the excitation energies are large by 0.1–0.2 eV, when compared to the relevant experiments.

IV. ELECTRON DYNAMICS IN A MOLECULAR WIRE

The real-time approach to time-dependent density functional theory opens new venues to handling problems where electron dynamics and correlation is important. For example, the method is applied to a molecular wire. Molecular wires[33,34] (MW) are essential building blocks of molecular size electronic devices. In the simplest form, they consist of a molecule connected to two metallic leads. When the leads are placed under a potential difference, an instantaneous electric current forms where electrons are transferred from one lead to the other, presumably through the molecule. The conductance of the MW depends in a complex way on the geometry, on the potential difference, and on the molecule itself.[34,35] Theoretical treatments of this system are mostly based on the Landauer expression,[36] usually made within a single electron approximation neglecting electron correlation.[37,38] With TDLDA, one can treat the system at an *ab initio* level considering electron correlation.

As an illustration, we take a simplified MW. Each electrode is modeled by a single gold atom, and the ethylene molecule (C_2H_4) is connected to each lead via a sulfur atom[35] (see Fig. 4). The coordinates of the atoms in the MW are given in Table II. The molecule is placed in a rectangular cell sampled by a grid of spacing δx (in each dimension).

Starting with the ground state density at $t=0$ a.u., an electric field directed along the Au–Au axis (the z-axis), is applied. The potential difference is linear along the molecular wire, and forced to zero beyond the gold atoms. The dynamics of the charge density is then followed in time.

The behavior of the density as a function of time can be inferred from the snapshots of the linear density along the z axis, shown in Fig. 5.

By a partial integration of the charge distribution, the total charge Q transferred from the left part of the molecule ($z<0$) to its right part ($z>0$) is determined, as shown in Fig. 6. It is seen that after a fast charge transfer, the charge distribution continues to oscillate in time.

We now construct a model to interpret these transients. As a result of the initial applied potential difference V_o, an amount of charge $Q(t)$ is transferred by time t from the left to the right atom. A counter electric field is then formed so that the total potential difference between the two electrodes is given by

$$V(t)=V_o-C^{-1}Q(t), \tag{18}$$

where C is an effective capacitance of the molecular wire. Assuming an effective resistance R, the current at time t is given by

$$RI(t)=V(t). \tag{19}$$

Equations (18) and (19) lead to a differential equation for the charge $Q(t)$. This equation is identical to that of an *RC* circuit, yielding a transferred charge of

$$Q(t)=CV_o(1-e^{-t/RC}). \tag{20}$$

The initial potential difference between the gold atoms is estimated from the electric field strength and their distance along the z axis

$$V_o=E(z_{\mathrm{Au1}}-z_{\mathrm{Au2}})=0.41\ \mathrm{V}. \tag{21}$$

By fitting the signal of Eq. (20) to the observed signal (see Fig. 6), one can determine the resistance 50 kΩ and capacitance 2×10^{-20} F of the MW. These results were found to be reasonably stable against change of grid spacing and box length, as shown in Table III. We should note that the charge transfer results are highly converged with respect to grid spacing at $\delta x=0.4$ a.u. This is seen clearly in Fig. 6, where curves B and C are practically indistinguishable. The convergence of the transients with cell size is slower, although the resistance and capacitance results are only slightly insensitive.

The calculated value of the resistance of a molecular wire is substantially smaller than that normally calculated for such structures (using Landauer formulas). This is because the resistance of a molecular fragment when it is adsorbed on a metal is fixed not only by the molecule itself but also by the density of states in the metal. The methodology developed here can in principle be applied to a larger portion of the metal, by adding more gold atoms. Such a procedure is conceptually simple, but very costly in terms of computational resources.

By changing the box size L_z and the grid spacing δx, the sensitivity of the results to these parameters can be assessed. It is seen in Fig. 6 and Table III that the results are converged to high accuracy when $\delta x=0.4$ bohr. Convergence with box size is slower but still seems reasonable.

V. SUMMARY

We have presented an accurate nonlinear time evolution scheme based on Chebyshev interpolation in the time domain. The equation set up is an implicit integral equation. The implicit nature of the method is prerequisite for a stable evolution. The solution of the nonlinear implicit equations is greatly accelerated by a DIIS[17] scheme.

In principle, the time steps T can be large; however, the number of sampling points is proportional to T (see the Appendix for a discussion) so that a very large value of T *is* penalized by increased memory demands. The iterations are harder to converge for very large time steps. We find a well-balanced method (in terms of memory vs time step) is one where the number of sampling points is low—around $N=5$ to $N=10$.

The high accuracy and reliability of the method is prerequisite for studying elaborate dynamical electronic processes, such as sub-femtosecond spectroscopy and various charge transfer processes. The merits of the method were demonstrated by computing adiabatic potential energy curves of Al_2. We have demonstrated that this approach enables studying complicated time-dependent electronic processes in systems such as molecular wires. Work in this direction will be undertaken in future studies.

ACKNOWLEDGMENTS

The authors thank R. Kosloff for comments and stimulating discussions. This research was supported by Grant No. 9800108 from the United States–Israel Binational Science Foundation (BSF), Jerusalem, Israel. We gratefully acknowledge the use of computational resources at the Fritz Haber center in the Hebrew University of Jerusalem and the High Performance Computing Unit of the Inter University Computation Center of Israel.

APPENDIX

The choice of the N sampling points t_n within a time interval $[0,T]$ and the interpolating functions $Q_m(t)$ $(n,m=0,...,N-1)$, for interpolating a time-dependent function $f(t)$ [using Eq. (6)], is now discussed. The sampling points and functions are connected by the interpolation property

$$Q_m(t_n)=\delta_{nm}. \tag{A1}$$

A correct choice of the interpolation points is crucial for the accuracy and efficiency of the method.

The starting point of our reasoning is the possibility of approximating a time-dependent function $f(t)$ using a Chebyshev polynomial expansion. For this purpose, let us define a function $\tilde{f}(x)=f((x+1)(T/2))$ on the interval $x\in[-1,1]$, and write the expansion as[39]

$$\tilde{f}(x)\approx\tilde{f}_N(x)=\sum_{k=0}^{N-1}F_kC_k(x). \tag{A2}$$

Here, $C_k(x)$ is the kth Chebyshev polynomial, obeying the following recursion relations:[39]

$$C_{k+1}=2xC_k-C_{k-1},\ C_0=1,\ C_1=x, \tag{A3}$$

and

$$F_k=\frac{2-\delta_{k0}}{\pi}\int_{-1}^{1}\frac{\tilde{f}(x)C_k(x)}{\sqrt{1-x^2}}dx, \tag{A4}$$

because the Chebyshev polynomials constitute an orthogonal family over the interval

$$\frac{2}{\pi}\int_{-1}^{1}\frac{C_n(x)C_m(x)}{\sqrt{1-x^2}}dx=\delta_{nm}(1+\delta_{n0}). \tag{A5}$$

The maximal error committed in truncating the expansion after N terms can be bounded[39]

$$\max_x|f(x)-f_N(x)|=|F_N|\max_x|C_N(x)|\leqslant|F_N|. \tag{A6}$$

For smooth functions, taking N to infinity causes the expansion to converge uniformly to the function over the interval. It can be proved that this expansion [Eqs. (A2) and (A4)] leads to the best converging polynomial approximation in the maximum norm.[39] This result is related to the fact that of all polynomials $p_N(x)=x^N+a_{N-1}x^{N-1}+\cdots+a_0$, the polynomial $2^{-N}C_N(x)$ is the smallest (maximum norm-wise) in the interval $[-1,1]$.

The intermediate conclusion is, that this procedure for approximating functions is a ''best-fit technique.'' We now add to this fact the concept of the Gaussian quadrature, also called ''quadrature of the highest degree of algebraic precision.''[40] This technique is applied to the integrals that define the expansion coefficients. The Gaussian quadrature theory implies that the following rank-N quadrature rule is exact for all polynomials of degree $2N-1$:[40]

$$\int_{-1}^{1} \frac{p(x)}{\sqrt{1-x^2}} dx \approx \frac{\pi}{N} \sum_{n=0}^{N-1} p(x_n), \tag{A7}$$

where the points x_n are N roots of the Nth Chebyshev polynomial $C_N(x)$, given explicitly by

$$x_n = -\cos\left(\frac{\pi(n+(1/2))}{N}\right),\ n=0,1,...,N-1. \tag{A8}$$

We first apply the Gaussian quadrature to the orthogonal relations of the Chebyshev polynomials [Eq. (A5)], obtaining a discretized orthogonal relation of order $n<N$

$$\sum_{n=0}^{N-1} C_k(x_n) C_{k'}(x_n) = \frac{N}{2-\delta_{k,0}} \delta_{k,k'}. \tag{A9}$$

Next, we apply it to the integrals defining the expansion coefficients, yielding the order-N discretized completeness relation, of the Chebyshev polynomials[39]

$$\sum_{k=0}^{N-1} \frac{2-\delta_{k0}}{N} C_k(x_n) C_k(x_{n'}) = \delta_{n,n'}. \tag{A10}$$

This last equation directly connects with Eqs. (6) and (A1), yielding the form of $Q_n(t) = \tilde{Q}_n((2t/T)-1)$, with

$$\tilde{Q}_n(x) = \sum_{k=0}^{N-1} \frac{2-\delta_{k0}}{N} C_k(x_n) C_k(x). \tag{A11}$$

Finally, plugging Eq. (A11) into Eq. (8) gives the integration weights

$$I_n(x) = \sum_{k=0}^{N-1} \frac{2-\delta_{k0}}{2N} C_k(x_n) S_k(x), \tag{A12}$$

with

$$S_k(x) = \int_{-1}^{x} C_k(x) dx. \tag{A13}$$

This integral can be evaluated analytically from the following recursion, derivable from Chebyshev polynomial properties:

$$(k+2) S_{k+1} = 2(x^2-1) C_k + (k-2) S_{k-1}, \tag{A14}$$

and

$$S_0 = x+1,\ S_1 = (x^2-1)/2. \tag{A15}$$

Putting all the pieces together, using Chebyshev sampling points [Eq. (A8)], together with sampling functions $Q_n(t)$ [Eq. (A11)] yields a representation which enjoys the following virtues:

(1) *Interpolative:* Exact at the sampling points;
(2) *Best fit (maximum norm-wise):* thus, it must be highly accurate *between* the sampling points too;
(3) *Chebyshev efficiency:* Enjoys the merit of being the *most efficient* expansion achieving the two goals above.

An important feature of this scheme is that it is global: within a given number N of sampling points, neither the location of the sampling points nor the form of the interpolation function $Q_n(t)$ is affected by the function $f(t)$ we are representing. This is what makes the integral equation evolution scheme above possible. However, N must be chosen large enough to ensure that the aliasing errors introduced by the discrete sampling are so small that their accumulation is slow. We show in another publication[15] the detailed considerations one makes in determining the number N. Here, we just quote the result

$$N = \frac{e}{4} \Omega T + N_r, \tag{A16}$$

where Ω is the largest (in absolute value) eigenvalue of the Hamiltonian, T is the length of the interval, and N_r is an additional number of points depending on the accuracy to be achieved in the computation. For good accuracy ($1e-8$ in energy conservation per step) $N_r = 5$.

[1] E. Runge and E. K. U. Gross, Phys. Rev. Lett. **52**, 997 (1984).
[2] W. Kohn and L. J. Sham, Phys. Rev. A **140**, 1133 (1964).
[3] R. Kosloff, Annu. Rev. Phys. Chem. **45**, 145 (1994).
[4] W. H. Press, S. A. Teukolsky, W. T. Vetterling, and B. P. Flannery, *Numerical Recipes in C* (Cambridge University Press, Cambridge, England, 1992).
[5] M. D. Feit, J. A. Fleck, and A. Steiger, J. Comput. Phys. **47**, 412 (1982).
[6] H. Jiang and X. S. Zhao, Chem. Phys. Lett. **319**, 555 (2000).
[7] Y. Miyamoto and O. Sugino, Phys. Rev. B **62**, 2039 (2000).
[8] C. Leforestier, R. H. Bisseling, C. Cerjan *et al.*, J. Comput. Phys. **94**, 59 (1991).
[9] R. Kosloff, J. Phys. Chem. **92**, 2087 (1988).
[10] P. Pfeifer and R. D. Levine, J. Chem. Phys. **79**, 5512 (1983).
[11] U. Peskin, R. Kosloff, and N. Moiseyev, J. Chem. Phys. **100**, 8849 (1994).
[12] G. H. Yao and R. E. Wyatt, J. Chem. Phys. **101**, 1904 (1994).
[13] G. H. Yao and R. E. Wyatt, Chem. Phys. Lett. **239**, 207 (1995).
[14] C. S. Guiang and R. E. Wyatt, Int. J. Quantum Chem. **67**, 273 (1998).
[15] R. Baer, Phys. Rev. A (in press).
[16] P. Henrici, *Discrete Variable Methods in Ordinary Differential Equations* (Wiley, New York, 1962).
[17] P. Pulay, Chem. Phys. Lett. **73**, 393 (1980).
[18] M. Petersilka, U. J. Gossmann, and E. K. U. Gross, Phys. Rev. Lett. **76**, 1212 (1996).
[19] D. J. Tozer and N. C. Handy, J. Chem. Phys. **109**, 10180 (1998).
[20] K. Yabana and G. F. Bertsch, Phys. Rev. B **54**, 4484 (1996).
[21] K. Yabana and G. F. Bertsch, Z. Phys. D: At., Mol. Clusters **42**, 219 (1997).
[22] K. Yabana and G. F. Bertsch, Phys. Rev. A **60**, 3809 (1999).
[23] K. Yabana and G. F. Bertsch, Int. J. Quantum Chem. **75**, 55 (1999).
[24] K. Yabana and G. F. Bertsch, Phys. Rev. A **60**, 1271 (1999).
[25] Z. W. Fu, G. W. Lemire, G. A. Bishea, and M. D. Morse, J. Chem. Phys. **93**, 8420 (1990).
[26] M. A. Douglas, R. H. Hauge, and J. L. Margrave, J. Phys. Chem. **87**, 2945 (1983).
[27] M. F. Cai, C. C. Carter, T. A. Miller, and V. E. Bondybey, Chem. Phys. **155**, 233 (1991).
[28] H. Basch, W. J. Stevens, and M. Krauss, Chem. Phys. Lett. **109**, 212 (1984).
[29] S. R. Langhoff and C. W. Bauschlicher, J. Chem. Phys. **92**, 1879 (1990).
[30] S. S. Han, H. Hettema, and D. R. Yarkony, J. Chem. Phys. **102**, 1955 (1995).
[31] N. Troullier and J. L. Martins, Phys. Rev. B **43**, 1993 (1991).
[32] M. Fuchs and M. Scheffler, Comput. Phys. Commun. **119**, 67 (1999).
[33] A. Aviram and M. A. Ratner, Chem. Phys. Lett. **29**, 257 (1974).
[34] V. J. Langlais, R. R. Schlittler, H. Tang, A. Gourdon, C. Joachim, and J. K. Gimzewski, Phys. Rev. Lett. **83**, 2809 (1999).
[35] M. A. Reed, C. Zhou, C. J. Muller, T. P. Burgin, and J. M. Tour, Science **278**, 252 (1997).

[36] R. Landauer, Philos. Mag. **21**, 863 (1970).
[37] E. G. Emberly and G. Kirczenow, Phys. Rev. B **58**, 10911 (1998).
[38] E. G. Emberly and G. Kirczenow, Mol. Electron. Science Technol. **852**, 54 (1998).
[39] T. J. Rivlin, *Chebyshev Polynomials: From Approximation Theory to Algebra and Numbers Theory* (Wiley, New York, 1990).
[40] V. I. Krylov, *Approximate Calculation of Integrals* (Macmillan, New York, 1962).